

# FIRST RESULTS FROM THE LYMAN ALPHA GALAXIES IN THE EPOCH OF REIONIZATION (LAGER) SURVEY: COSMOLOGICAL REIONIZATION AT $Z \sim 7$

ZHEN-YA ZHENG<sup>1,2,3</sup>, JUNXIAN WANG<sup>4</sup>, JAMES RHOADS<sup>5,6</sup>, LEOPOLDO INFANTE<sup>1</sup>, SANGEETA MALHOTRA<sup>5,6</sup>, WEIDA HU<sup>4</sup>, ALISTAIR R. WALKER<sup>7</sup>, LINHUA JIANG<sup>8</sup>, CHUNYAN JIANG<sup>2,3,9</sup>, PASCALE HIBON<sup>10</sup>, ALICIA GONZALEZ<sup>5</sup>, XU KONG<sup>4</sup>, XIANZHONG ZHENG<sup>11</sup>, GASPAR GALAZ<sup>1</sup>, FELIPE L. BARRIENTOS<sup>1</sup>.

<sup>1</sup>Institute of Astrophysics and Center for Astroengineering, Pontificia Universidad Catolica de Chile, Santiago 7820436, Chile; zhengzy@shao.ac.cn, linfante@astro.puc.cl

<sup>2</sup>CAS Key Laboratory for Research in Galaxies and Cosmology, Shanghai Astronomical Observatory, Shanghai 200030, China;

<sup>3</sup>Chinese Academy of Sciences South America Center for Astronomy, Santiago 7591245, Chile

<sup>4</sup>CAS Key Laboratory for Research in Galaxies and Cosmology, Department of Astronomy, University of Science and Technology of China, Hefei, Anhui 230026, China; jxw@ustc.edu.cn

<sup>5</sup>School of Earth and Space Exploration, Arizona State University, Tempe, AZ 85287, USA; Sangeeta.Malhotra@asu.edu, James.Rhoads@asu.edu

<sup>6</sup>Astrophysics Science Division, Goddard Space Flight Center, 8800 Greenbelt Road, Greenbelt, Maryland 20771, USA;

<sup>7</sup>Cerro Tololo Inter-American Observatory, Casilla 603, La Serena, Chile

<sup>8</sup>The Kavli Institute for Astronomy and Astrophysics, Peking University, Beijing, 100871, China

<sup>9</sup>Núcleo de Astronomía, Facultad de Ingeniería y Ciencias, Universidad Diego Portales, Av. Ejército 441, Santiago, Chile

<sup>10</sup>European Southern Observatory, Alonso de Cordova 3107, Casilla 19001, Santiago, Chile

<sup>11</sup>Purple Mountain Observatory, Chinese Academy of Sciences, Nanjing 210008, China

*Draft version March 10, 2017*

## ABSTRACT

We present the first results from the ongoing LAGER project (Lyman Alpha Galaxies in the Epoch of Reionization), which is the largest narrowband survey for  $z \sim 7$  galaxies to date. Using a specially built narrowband filter NB964 for the superb large-area Dark-Energy Camera (DECAM) on the NOAO/CTIO 4m Blanco telescope, LAGER has collected 34 hours NB964 narrowband imaging data in the 3 deg<sup>2</sup> COSMOS field. We have identified 27 Lyman Alpha Emitter (LAE) candidates at  $z = 6.9$  in the central 2-deg<sup>2</sup> region, where DECAM and public COSMOS multi-band images exist. The resulting luminosity function can be described as a Schechter function modified by a significant excess at the bright end (4 galaxies with  $L_{Ly\alpha} \sim 10^{43.4 \pm 0.2}$  erg s<sup>-1</sup>). The number density at  $L_{Ly\alpha} \sim 10^{43.4 \pm 0.2}$  erg s<sup>-1</sup> is little changed from  $z = 6.6$ , while at fainter  $L_{Ly\alpha}$  it is substantially reduced. Overall, we see a fourfold reduction in Ly $\alpha$  luminosity density from  $z = 5.7$  to 6.9. Combined with a more modest evolution of the continuum UV luminosity density, this suggests a factor of  $\sim 3$  suppression of Ly $\alpha$  by radiative transfer through the  $z \sim 7$  intergalactic medium (IGM). It indicates an IGM neutral fraction  $x_{HI} \sim 0.4$ – $0.6$  (assuming Ly $\alpha$  velocity offsets of 100–200 km s<sup>-1</sup>). The changing shape of the Ly $\alpha$  luminosity function between  $z \lesssim 6.6$  and  $z = 6.9$  supports the hypothesis of ionized bubbles in a patchy reionization at  $z \sim 7$ .

*Keywords:* cosmology: observations — dark ages, reionization, first stars — galaxies: high-redshift — galaxies: luminosity function, mass function

## 1. INTRODUCTION

In the last decade, much progress has been made in narrowing down the epoch of cosmological reionization to be between  $z \sim 6$  (Ly $\alpha$  saturation in  $z \sim 6$  quasar, Fan et al. 2006) and  $z \sim 9$  (Polarization of CMB photons, Planck results XIII 2015). In between, quasars, gamma ray bursts (GRBs), and galaxies at  $z \gtrsim 6$  are important to constrain the nature of reionization. However, the rarity of high- $z$  quasars (with only one known at  $z \gtrsim 7$ , Bolton et al. 2011), and of high- $z$  GRBs with rapid followup, limit their application as reionization probes. In contrast, hundreds of galaxies at  $z \gtrsim 6$  have been reported from ground-based narrowband Ly $\alpha$  line searches (e.g., Ouchi et al. 2010), from space-based broadband Lyman break searches (e.g., Bouwens et al. 2015; Finkelstein et al. 2015), and from newly taken space-based grism spectroscopic surveys (Tilvi et al. 2016; Bagley et al. 2017). Their luminosities, number densities, clustering, and ionizing powers are essential to probe the epoch of reionization (EoR).

Because Ly $\alpha$  photons are resonantly scattered by neutral hydrogen, Ly $\alpha$  emitters (LAEs) provide a sensitive, practical, and powerful tool to determine the epoch, duration, and inhomogeneities of reionization. With a sample of LAEs in EoR, the easiest Ly $\alpha$  reionization test is the luminosity function (LF) test. Rhoads & Malhotra (2001) first applied this test at  $z = 5.7$ , then at 6.5 (Malhotra & Rhoads 2004; Stern et al. 2005). Subsequent surveys have confirmed and refined the  $z = 6.5$ – $6.6$  neutral fraction measurement to  $x_{HI} \lesssim 0.3$  (Ouchi et al. 2010; Kashikawa et al. 2011), and have found a significant neutral fraction increase from  $z = 6.6$  to  $z = 7.3$  (Konno et al. 2014). Other implementations of Ly $\alpha$  reionization tests include the Ly $\alpha$  visibility test (Jensen et al. 2013; Schenker et al. 2014), i.e., the Ly $\alpha$  fraction in LBGs in EoR, the volume test (Malhotra & Rhoads 2006, Rhoads & Malhotra 2017, in prep.), i.e., each Ly $\alpha$  galaxy is taken as evidence for a certain volume of ionized gas, and the clustering test, e.g., the signature of a patchy partially-ionized

IGM is sought by looking for excess spatial correlations in the Ly $\alpha$  galaxy distribution (Furlanetto et al. 2006; McQuinn et al. 2007; Jensen et al. 2013).

Redshift  $z \gtrsim 7$  is the frontier in Ly $\alpha$  and re-ionization studies. Many searches for LAEs at  $z = 6.9$ – $7.0$  (Iye et al. 2006; Ota et al. 2008, 2010; Hibon et al. 2011, 2012),  $z = 7.2$ – $7.3$  (Shibuya et al. 2012; Konno et al. 2014), and  $z = 7.7$  (Hibon et al. 2010; Tilvi et al. 2010; Krug et al. 2012) have yielded  $\sim$  two dozen narrowband-selected candidates, but only 3 of these have been spectroscopically confirmed so far (Iye et al. 2006; Rhoads et al. 2012; Shibuya et al. 2012). In comparison, hundreds of LAEs have been found at lower redshift, at  $z = 6.6$  (e.g., Hu et al. 2010; Ouchi et al. 2010; Kashikawa et al. 2011; Matthee et al. 2015), and a large fraction of them have been spectroscopically confirmed (i.e., Kashikawa et al. 2011). The comoving volumes of the searches for  $z \gtrsim 7$  LAEs are all less than  $5 \times 10^5$  cMpc $^3$ , and some of the surveys with 200Å wide filters in the far-red inevitably include one or two weak OH emission lines, limiting their sensitivity. Thus, there is an urgent need for a systematic survey at  $z \sim 7$  with sufficient volume and depth to determine if the Ly $\alpha$  line is attenuated due to neutral IGM in a statistically significant way.

In this *Letter*, we report the discovery of a population of candidate  $z \sim 7$  Ly $\alpha$  emitters in the first field (COSMOS) of the Lyman-Alpha Galaxies in the Epoch of Reionization (LAGER) survey. With LAGER-COSMOS, we have the largest sample to date of candidate  $z \sim 7$  LAEs. In § 2, we describe the observation and data reduction of LAGER, then introduce the candidates selection method. In § 3, we present the candidates and their Ly $\alpha$  LF at  $z \sim 7$ . In § 4, we discuss the implications of these discoveries for *EoR* at  $z \sim 7$ .

## 2. SURVEY DESCRIPTION AND DATA

### 2.1. LAGER Survey

The LAGER survey is the largest narrowband survey yet for LAEs at  $z \gtrsim 7$ . It is currently ongoing, using the Dark Energy Camera (DECam, with FOV  $\sim 3$  deg $^2$ ) on the NOAO-CTIO 4m Blanco telescope together with an optimally designed custom narrowband filter NB964<sup>1</sup> (Central wavelength  $\sim 9642$ Å, FWHM  $\sim 90$ Å). LAGER is designed to select more than a hundred  $z \sim 7$  LAEs over an area of 12 deg $^2$  in 4 fields ( $8 \times 10^6$  cMpc $^3$ ). Currently, LAGER has collected 47 hrs NB964 narrowband imaging in 3 fields (CDF-S, COSMOS, and DLS-f5) taken during 9 nights in 2015 December, 2016 February, March and November.

The deepest NB964 imaging is done in COSMOS, where we have obtained 34 hours' NB964 exposure in a 3 deg $^2$  field. The exposure time per NB964 frame is 900s. Consecutive exposures were dithered by  $\sim 100''$  so that chip gaps and bad pixels do not lead to blank areas in the final stacks. We also took  $\sim 0.5$ – $1$  hrs  $z$  and  $Y$  bands exposure per field to exclude possible transients. There are deep archival DECam and Subaru broadband images in COSMOS.

<sup>1</sup> Please see the filter information at NOAO website: <http://www.ctio.noao.edu/noao/content/Properties-N964-filter>

### 2.2. Data Reduction and Analysis

We downloaded the reduced and calibrated DECam re-sampled images from the NOAO Science Archive, which were processed through the NOAO Community Pipeline (version 3.7.0, Valdes et al. 2014). The individual frames were stacked following the weighting method in Annis et al. (2014) with *SWarp* (version 2.38.0, Bertin 2010). The seeing of the final stacked LAGER-COSMOS narrowband image is  $0.93''$ .

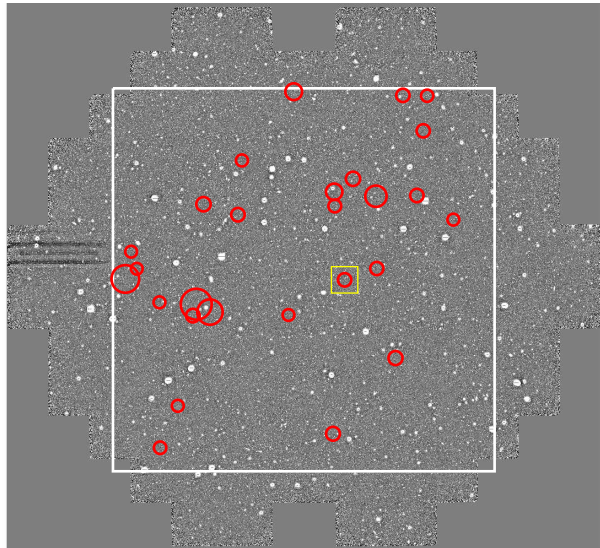


**Figure 1.** The DECam NB964 COSMOS field showing uneven distribution of candidate  $z \sim 7$  LAEs. The DECam NB964 area is  $\sim 3$  deg $^2$ , and the overlap region with Subaru Suprime-cam multi-band images is the central 2 deg $^2$  area in the white box. We have selected 27 candidate  $z \sim 7$  LAEs, which are marked in red circles with aperture sizes scaled to their Ly $\alpha$  line fluxes and normalized to  $\sim 1$  pMpc for the brightest LAE. The only spectroscopically confirmed LAE from previous narrowband survey (Rhoads et al. 2012) in this field is recovered and marked by a yellow box.

The zero-magnitudes of the DECam images were calibrated to the Subaru Suprime-Cam broadband magnitudes of the stars in the public COSMOS/UltraVISTA  $K_S$ -selected catalog (Muzzin et al. 2013). We estimated the image depth by measuring the root mean square (rms) of the background in blank places where detected ( $> 3\sigma$ ) signals were masked out. In a 2" diameter aperture, the  $3\sigma$  limiting AB magnitudes of the DECam images are  $[u, g, r, i, z, Y, \text{NB964}]_{3\sigma} = [26.2, 27.4, 26.9, 26.6, 26.1, 24.3, 25.6]$ . In the central 2-deg $^2$  area covered with Subaru Suprime-Cam optical deep images, their  $3\sigma$  limiting magnitudes within a 2" diameter aperture are  $[B, g', V, r', i', z', \text{NB711, NB816, NB921}]_{3\sigma} \sim [27.9, 27.6, 27.2, 27.4, 27.3, 25.9, 26.0, 26.1, 26.2]$ . These Subaru Suprime-Cam images are deeper and have better seeing than the DECam images on average.

We calculated the narrowband completeness via a Monte Carlo simulation. The completeness fraction is defined as the *SExtractor* recovery percentage of the randomly distributed artificial sources in NB964 image as a function of narrowband magnitude. The narrowband NB964 aperture magnitudes corresponding to the 80%, 50% and 30% completeness fractions are 24.2, 25.0, and 25.3, respectively.

### 2.3. Selection Criteria for $z \sim 7$ LAEs

Since Subaru broadband images are deeper and have better seeings than the DECam broadband images, we better apply selection criteria for  $z \sim 7$  LAEs in the central 2-deg<sup>2</sup> area covered by both Suprime-Cam and DECam. The selection criteria for  $z \sim 7$  LAEs include narrowband NB964 with  $>5\text{-}\sigma$  detection ( $\text{NB964} \leq \text{NB964}_{5\sigma} = 25.07$ ), narrowband NB964 excess over broadband  $z$  ( $z - \text{NB964} \geq 1.0$ ), and non-detections in both DECam  $ugri$  and Suprime-Cam  $Bg'VRi'$ , N711, N816, N921 bands. We specially exclude broadband detections in the  $1''.08$  (4 pixel) diameter aperture to exclude marginal signals in these bands. 156 sources passed the selection criteria, but a large fraction of them are fake sources (bleed trails, diffraction spikes, etc) after our visual check on NB964 image.

## 3. RESULTS

### 3.1. Candidate LAEs at $z \sim 7$ in LAGER-COSMOS

In total, 27 candidate  $z \sim 7$  LAEs are selected, after our team's tripartite visual check on both NB964 and broadband images to exclude artificial ones. The positions of these candidates are plotted in Figure 1. Their Ly $\alpha$  line fluxes, derived from narrowband and  $z$ -band photometry<sup>2</sup>, are in the range of  $0.7\text{--}7 \times 10^{-17}$  erg cm<sup>-2</sup> s<sup>-1</sup>. The corresponding observed Ly $\alpha$  line luminosities are  $4\text{--}40 \times 10^{42}$  erg s<sup>-1</sup>.

The 4 brightest of them, with  $L(\text{Ly}\alpha) = 16\text{--}40 \times 10^{42}$  erg s<sup>-1</sup>, are the most luminous candidate LAEs known at  $z \gtrsim 7$ , thanks to the large survey volume of LAGER.

One of the candidates, J09:59:50.99+02:12:19.1, was previously selected and spectroscopically confirmed as a  $z = 6.944$  LAE with Magellan IMACS narrowband imaging and spectroscopy over a much smaller field (Rhoads et al. 2012). It is well recovered with our selection using new DECam narrowband imaging.

**Table 1**

Ly $\alpha$  luminosity function at  $z \sim 7$  in the LAGER-COSMOS field.

$\log(L_i)$ ( $\Delta L=0.14$ )	$N \pm \Delta N^\dagger$ [ $L_i \pm \frac{\Delta L}{2}$ ]	$f_{\text{comp.}}$	$\text{Log}_{10} \Phi(L_i)$ [ $(d\text{Log}_{10} L)^{-1} \text{Mpc}^{-3}$ ]
42.63	$6^{+3.6}_{-2.4}$	0.20	$-3.77^{+0.20}_{-0.22}$
42.77	$9^{+4.1}_{-2.9}$	0.43	$-3.93^{+0.16}_{-0.17}$
42.91	$6^{+3.6}_{-2.4}$	0.64	$-4.27^{+0.20}_{-0.22}$
43.05	$2^{+2.7}_{-1.3}$	0.76	$-4.82^{+0.37}_{-0.45}$
43.19	$< 2.6$	0.81	$< -4.73$
43.33	$1^{+2.3}_{-0.8}$	0.87	$-5.19^{+0.52}_{-0.77}$
43.47	$2^{+2.7}_{-1.3}$	0.91	$-4.90^{+0.37}_{-0.45}$
43.61	$1^{+2.3}_{-0.8}$	0.95	$-5.22^{+0.52}_{-0.77}$

<sup>†</sup>: 1-sigma Poisson errors (Gehrels 1986).

### 3.2. Ly $\alpha$ Luminosity Function at $z \sim 7$

<sup>2</sup>  $F_{\text{Ly}\alpha} \equiv \frac{W_z F_{\text{NB}} - W_{\text{NB}} F_z}{W_z - W_{\text{NB}}}$ , where F and W are the band total flux and width, respectively.

We use the  $V/V_{\text{max}}$  method to calculate the Ly $\alpha$  LF at  $z = 6.9$ . The formula below is adopted:

$$\Phi(L)dL = \sum_{L-dL/2 \leq L_i \leq L+dL/2} \frac{1}{V_{\text{max}}(L_i) \times f_{\text{comp}}(L_i)}. \quad (1)$$

Here  $V_{\text{max}}(L_i)$  is the maximum survey volume for LAEs with Ly $\alpha$  luminosity  $L_i$ , and  $f_{\text{comp}}(L_i)$  is the narrowband detection completeness (see §2.2) at  $L_i$ .

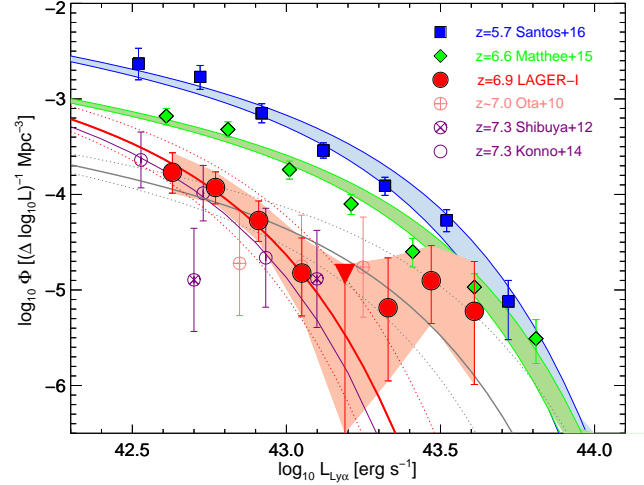


**Figure 2.** The Ly $\alpha$  LFs of LAE surveys at  $z \sim [5.7, 6.6, 7, 7.3]$ . The red filled circles show our results at  $z \sim 7$  from LAGER-COSMOS field. References: Ly $\alpha$  LF at  $z = 5.7$  from Santos et al. (2016) (blue filled squares), at  $z = 6.6$  from Matthee et al. (2015) (green filled diamonds), at  $z \sim 7$  from Ota et al. (2010) (pink empty circles with plus), and at  $z = 7.3$  from Shibuya et al. (2012) (purple empty circles with cross) and Konno et al. (2014) (purple empty circles). The colored regions in blue and green show the best Schechter fit with  $\pm 1\sigma$  error in  $L^*$  at  $z \sim 5.7$  and  $6.5$ , respectively, from Santos et al. (2016). The solid and dashed lines in red (gray) show the best Schechter fit with the  $\pm 1\sigma$  error in  $L^*$  at  $z \sim 6.9$  with  $L$  range  $42.6 \leq \log(L) \leq 43.2$  ( $42.6 \leq \log(L) \leq 43.6$ ) (see Table 2). The purple line shows the best Schechter fit at  $z \sim 7.3$  from Konno et al. (2014).

The Ly $\alpha$  LF of LAEs at  $z \sim 7$  in the LAGER-COSMOS field is listed in Table 1, and plotted in Figure 2 together with LAE LFs at  $z \sim 5.7\text{--}7.3$  from literature. The LF shows dramatic evolution not only in normalization, but also in the shape.

The faint end of our LF ( $42.6 \leq \log_{10} L_{\text{Ly}\alpha} \leq 43.2$ ) at  $z \sim 7$  can be fitted with a single Schechter function in the form of

$$\Phi(L)dL = \Phi^* \left(\frac{L}{L^*}\right)^\alpha \exp\left(-\frac{L}{L^*}\right) d\left(\frac{L}{L^*}\right). \quad (2)$$

Because our survey does not go far below  $L^*$ , we fix  $\alpha = -1.5$  in our fitting. We find a large drop in LAE density, compared with  $z = 5.7$  and  $z = 6.6$ . Our result is statistically consistent with the measurement at  $z = 7.3$ . The best-fit Schechter function parameters of these LFs are listed in Table 2, and plotted in the upper panel of Figure 3.

More strikingly, we see a clear bump, i.e., significant excess to the Schechter function in the bright end of our  $z \sim 7$  LF ( $\log_{10} L_{\text{Ly}\alpha} \gtrsim 43.2$ ). It demonstrates that, while

the space density of faint LAEs drops tremendously from  $z = 5.7$  and  $6.6$  to  $z = 6.9$ , that of the luminous ones shows at most a mild change. Similarly but much less prominently, the LF evolution between  $z = 5.7$  and  $z = 6.6$  appears also differential, with a significant decline at the faint end but no clear evolution at the bright end (Matthee et al. 2015; Santos et al. 2016).

#### 4. DISCUSSION

##### 4.1. The Evolution of Ly $\alpha$ LF in EoR

Cosmological reionization was well under way by  $z \sim 9$  (Planck results XIII 2015), and ended by  $z \sim 6$  (Fan et al. 2006). Ly $\alpha$  galaxies at  $z \gtrsim 6$ , e.g., from LAE surveys at  $z = 5.7$  (Ouchi et al. 2008; Santos et al. 2016), at  $z = 6.6$  (Ouchi et al. 2010; Matthee et al. 2015), at  $z = 6.9$  (our LAGER-COSMOS sample), and at  $z = 7.3$  (Konno et al. 2014), are unique samples useful to probe both galaxy evolution and reionization.

In this work, we detect for the first time a significant bump at the bright end of Ly $\alpha$  LF at  $z \gtrsim 7$ . Previous surveys for LAEs at  $z \gtrsim 7$  failed to reveal it as they covered much smaller volumes.

The existence of such bright end bump is consistent with the scenario proposed by Haiman & Cen (2005), that bright LAEs are less attenuated by a neutral IGM than faint LAEs, as the larger Strömgren sphere surrounding luminous LAEs alleviates the neutral IGM absorption (also see Matthee et al. 2015, particularly their Fig. 8). Therefore, the evolution in the bright end of the LF better reflects the intrinsic evolution of LAEs, while the faint end is controlled by the evolution of both galaxies and the IGM.

The bottom panel of Figure 3 shows the evolution of luminosity densities both for Ly $\alpha$  and UV photons. Compared to LBGs (yellow shaded region), an accelerated evolution of LAE Ly $\alpha$  densities from  $z = 6.6$  (green diamonds) to  $z = 7.3$  (purple cross), as reported by Konno et al. (2014), is clearly seen in Figure 3. Since UV photons detected in LBGs are insensitive to the neutral hydrogen in EoR, Konno et al. (2014) concluded that such rapid evolution in LAE LFs can be attributed to a large neutral IGM fraction at  $z \sim 7.3$ . Our LAGER survey shows rapid evolution from  $z = 6.6$  to  $6.9$ , and a much smaller difference between  $z = 6.9$  and  $7.3$  (see Figure 3). It is possible that the evolution in the neutral fraction accelerated after  $z = 6.9$ , though a smooth, monotonic neutral fraction evolution  $5.7 \leq z \leq 7.3$  also fits the LAGER results and Konno et al. (2014) measurements within their uncertainties. Note that the cosmic time from  $z \sim 6.6$  to  $6.9$  and from  $z \sim 6.9$  to  $7.3$  are approximately equal, which is about 50 Myr.

Furthermore, compared to the evolution of Ly $\alpha$  densities  $\rho_{Ly\alpha}$  between redshifts of  $5.7$  and  $6.9$ , the evolution in the bright end only  $\rho_{Ly\alpha}^{\text{Bright}}$  follows a much smoother trend, somehow similar to but still steeper than the UV densities of LBGs (bottom panel of Figure 3). This demonstrates that either the intrinsic LAE LF evolves moderately between  $z=5.7$  and  $6.9$ , or IGM attenuation plays a role even at the highest luminosity bin. Consequently, the dramatic and rapid evolution between  $z = 6.6$  and  $6.9$  in the faint end can be mainly attributed to the change of neutral IGM fraction. This is also consistent with the spectroscopic Ly $\alpha$  visibility test, where

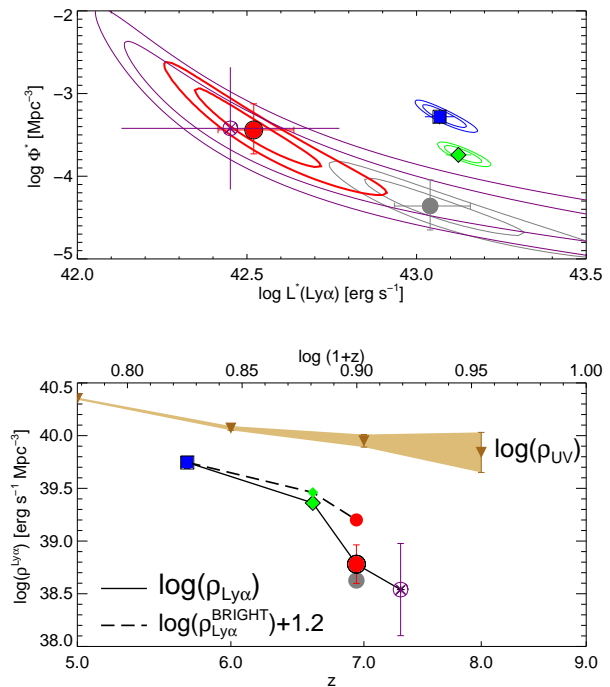


**Figure 3.** *Top:* The evolution of best-fit schechter parameters  $L_{Ly\alpha}^*$  and  $\Phi_{Ly\alpha}^*$  of Ly $\alpha$  LFs at  $z = [5.7, 6.6, 6.9, 7.3]$  with 1 and 2  $\sigma$  error contours. *Bottom:* Evolution of Ly $\alpha$  and UV luminosity densities at  $z \gtrsim 6$ . We plot the Ly $\alpha$  luminosity densities integrated over the best-fit Schechter functions ( $\log_{10} L_{Ly\alpha} > 42.4$ , see Figure 2), and for the brightest only ( $43.4 \lesssim \log_{10} L_{Ly\alpha} \lesssim 43.7$ ). Note the bright luminosity density is scaled up by 1.2 dex. The yellow shaded region represents the UV luminosity densities for  $L_{UV} > 0.03 L_{UV}^*$  given by Finkelstein et al. (2015) at  $z \sim 5.0, 6.0, 7.0$  and  $8.0$ . The symbols are the same as those in Figure 2.

LBGs at  $z \sim 7$  show a large drop in the fraction of visible Ly $\alpha$  lines (e.g., Schenker et al. 2014)

##### 4.2. Neutral IGM fraction at $z \sim 7$ with LAGER

Following Ouchi et al. (2010) and Konno et al. (2014), we compare the Ly $\alpha$  luminosity densities at  $z = 6.9$  (in EoR) and at  $z = 5.7$  (when reionization is completed) to estimate the effective IGM transmission factor  $T_{Ly\alpha, z}^{\text{IGM}}$ . Assuming the stellar population, ISM, and dust are similar at  $z = 6.9$  and  $z = 5.7$ , we obtain

$$T'_{z=6.9} = \frac{T_{Ly\alpha, z=6.9}^{\text{IGM}}}{T_{Ly\alpha, z=5.7}^{\text{IGM}}} = \frac{\rho_{z=6.9}^{Ly\alpha, tot} / \rho_{z=5.7}^{Ly\alpha, tot}}{\rho_{z=6.9}^{\text{UV}} / \rho_{z=5.7}^{\text{UV}}}. \quad (3)$$

Here  $\rho^{\text{UV}}$  and  $\rho^{\text{Ly}\alpha}$  are UV and Ly $\alpha$  luminosity densities, respectively. The ratio of UV luminosity densities  $\rho_{z=6.9}^{\text{UV}} / \rho_{z=5.7}^{\text{UV}} = 0.63$  is obtained from Finkelstein et al. (2015). From Table 2, we obtain the ratio of total Ly $\alpha$  luminosity densities  $\rho_{z=6.9}^{Ly\alpha, tot} / \rho_{z=5.7}^{Ly\alpha, tot} = 0.22$ . Thus we estimate  $T'_{z=6.9} = 0.35$  (c.f.,  $T'_{z=7.3} = 0.29$  from Konno et al. 2014).

Converting the Ly $\alpha$  emission line transmission factor to neutral IGM fraction  $x_{HI}$  is model dependent (e.g., Santos 2004; McQuinn et al. 2007; Dijkstra et al. 2007). An important factor is the shift of the Ly $\alpha$  line with respect to the systemic velocity, which is widely observed and may be explained by Ly $\alpha$  radiative transfer in a

**Table 2**  
Best-fit Schechter parameters and Ly $\alpha$  luminosity densities.

Redshift (1)	Volume (2) $\times 10^9 \text{ Mpc}^3$	$L(\text{Ly}\alpha)$ Range (3)	$\log_{10}[L_{\text{Ly}\alpha}^*]$ (4) [ $\text{erg s}^{-1}$ ]	$\log_{10}[\Phi^*]$ (5) [ $\text{Mpc}^{-3}$ ]	$\log_{10}[\rho_{\text{Ly}\alpha}]^\dagger$ (6) [ $\text{erg s}^{-1} \text{ Mpc}^{-3}$ ]	$\log_{10}[\rho_{\text{Ly}\alpha}]^\ddagger$ (7) [ $\text{erg s}^{-1} \text{ Mpc}^{-3}$ ]	$\log_{10}[\rho_{\text{Ly}\alpha}^{\text{Bright}}]^\ddagger$ (8)	Reference (9)
			Two free parameters $L_{\text{Ly}\alpha}^*$ and $\Phi^*$ with fixed $\alpha = -1.5$					
5.7	63.0	42.4–43.7	43.06 $\pm$ 0.05	-3.25 $\pm$ 0.09	40.06 $\pm$ 0.06	39.69 $\pm$ 0.06	38.6	Santos et al. (2016)
6.6	42.6	42.5–43.8	43.12 $\pm$ 0.04	-3.73 $\pm$ 0.07	39.64 $\pm$ 0.03	39.37 $\pm$ 0.03	38.3	Matthee et al. (2015)
6.9	12.6	<b>42.6–43.6</b>	43.04 $^{+0.17}_{-0.12}$	-4.36 $\pm$ 0.21	38.93 $\pm$ 0.16	38.63 $\pm$ 0.16	38.0	This study
		<b>42.6–43.2</b>	42.56 $^{+0.12}_{-0.11}$	-3.40 $^{+0.32}_{-0.29}$	39.41 $\pm$ 0.18	38.79 $\pm$ 0.18	–	This study
7.3	2.5	42.4–43.0	42.45 $\pm$ 0.32	-3.42 $\pm$ 0.74	39.28 $\pm$ 0.44	38.54 $\pm$ 0.44	–	Konno et al. (2014)

$\dagger$ : Ly $\alpha$  luminosity densities integrated over the best-fit Schechter functions at  $L_{\text{Ly}\alpha} \geq 0 \text{ erg s}^{-1}$  (column-6) and at  $L_{\text{Ly}\alpha} \geq 10^{42.4} \text{ erg s}^{-1}$  (column-7).

$\ddagger$ : Ly $\alpha$  luminosity densities for the brightest only ( $10^{43.4} \leq L_{\text{Ly}\alpha} \leq 10^{43.7}$ , column-8).

galactic wind or outflow. The Ly $\alpha$  velocity shift measurements of  $z \sim 6$ –7 galaxies are very limited and are mostly around 100–200  $\text{km s}^{-1}$  (Stark et al. 2015, 2017; Pentericci et al. 2016, but see two UV luminous galaxies with 400–500  $\text{km s}^{-1}$  reported by Willott et al. 2015). With the analytic model of Santos (2004), assuming a Ly $\alpha$  velocity shift of 0 and 360  $\text{km s}^{-1}$ , the value of  $T'_{z=6.9} = 0.30$  corresponds to  $x_{\text{HI}} \sim 0.0$  and 0.7 respectively.

By comparing our observed Ly $\alpha$  LF at  $z = 6.9$  to that predicted with the radiative transfer simulations by McQuinn et al. (2007, their Fig. 4), we obtain  $x_{\text{HI}} \sim 0.4$ –0.6 at  $z = 6.9$ . Similar results are obtained in the analytic studies considering ionization bubbles (Furlanetto et al. 2006; Dijkstra et al. 2007). We should note that these studies predicted a suppression of the luminosity function that is rather uniform across a wide range of luminosities (e.g., Sec. 4 of McQuinn et al. 2007). This suggests that the true distribution of ionized region sizes may differ appreciably from those used in literature (Furlanetto et al. 2006; Dijkstra et al. 2007; McQuinn et al. 2007). We conclude that the neutral hydrogen fraction is  $x_{\text{HI}} \sim 0.4$ –0.6 at  $z = 6.9$ . The range of  $x_{\text{HI}}$  value is caused by the uncertainties in the models.

#### 4.3. Ionized Bubbles at $z \sim 7$

The bump at the bright end of the Ly $\alpha$  LF is an indicator of large enough ionized bubbles, where the Hubble flow and galactic inflow/outflow can bring Ly $\alpha$  photons out of resonance, thus leading to different evolution of Ly $\alpha$  LF at the bright end and the faint end. The uneven distribution of these LAEs (Figure 1) may indicate a patchy reionization at  $z \sim 7$ . Larger LAGER samples in future will more definitely establish whether the degree of clustering in Figure 1 requires patchy reionization.

From the introduction section of Malhotra & Rhoads (2006), which gave the proper radius of a Strömgren sphere and the Gunn-Peterson effect optical depth of a LAE with outflow velocity  $\Delta V$  in  $EoR$ , we know that even the brightest LAE can not produce a large enough ionized bubble to effectively reduce the optical depth to  $\tau \sim 1$ . We would expect that some additional sources of photons must be associated with the bright LAEs, or these bright LAEs have very large Ly $\alpha$  offset velocities. It is possible that these bright LAEs are candidates of faint Active Galactic Nuclei (AGN) or direct collapse black holes.

From Figure 1, we do see some additional galaxies associated with the bright LAEs. However, we can not go deeper to find fainter LAEs with LAGER, and the clustering of LAEs at  $z \sim 7$  is beyond the topic of this letter. Future deep narrowband imaging with Subaru would resolve more additional faint galaxies associated with the bright LAEs.

Till now, only eight Ly $\alpha$  velocity offsets at  $z \gtrsim 6$  were reported by comparing Ly $\alpha$  line with UV line CIII]1909 (Stark et al. 2015, 2017) or FIR line [CII] (Pentericci et al. 2016; Willott et al. 2015). Among these, only two LBGs, which are among the brightest rest-frame UV luminous LBGs at  $z \gtrsim 6$ , have large Ly $\alpha$  offsets of 430 $\pm$ 69  $\text{km s}^{-1}$  and 504 $\pm$ 52  $\text{km s}^{-1}$  (Willott et al. 2015). Future NIR and/or FIR spectroscopic observation will help us to measure the Ly $\alpha$  velocity offsets of LAGER bright LAEs, and check the feature of faint AGN or direct collapse black holes.

## 5. CONCLUSION

In this letter, we report the first results of our LAGER project, the discovery of 27 (26 new) candidate LAEs at  $z \sim 7$ . This is the largest sample to date of candidate LAEs at  $z \gtrsim 7$ . Further more, thanks to the large survey volume of LAGER, we find 4 most luminous candidate LAEs at  $z \sim 7$  with  $L(\text{Ly}\alpha) = 16$ –40 $\times 10^{42} \text{ erg s}^{-1}$ . Compared to previous Ly $\alpha$  luminosity functions at  $z \gtrsim 6$ , the Ly $\alpha$  luminosity function of LAGER LAEs at  $z \sim 7$  shows different evolution at the faint-end and at the bright-end, which indicates a large neutral hydrogen fraction  $x_{\text{HI}} \sim 0.4$ –0.6 and the existence of ionized bubbles at  $z \sim 7$ . Our findings support the patchy reionization scenario at  $z \sim 7$ .

We acknowledge financial support from National Science Foundation of China (grants No. 11233002 & 11421303) and Chinese Top-notch Young Talents Program for covering the cost of the NB964 narrowband filter. J.X.W. thanks support from National Basic Research Program of China (973 program, grant No. 2015CB857005), and CAS Frontier Science Key Research Program QYCDJ-SSW-SLH006. Z.Y.Z acknowledges supports by the China-Chile Joint research fund 2015 and the CAS Pioneer Hundred Talents Program (C). L.I. is in part supported by CONICYT-Chile grants Basal- CATA PFB-06/2007, 3140542 and Conicyt-PIA-

ACT 1417. C.J. acknowledges support by Shanghai Municipal Natural Science Foundation (15ZR1446600)

We thank the engineers of Materion company for the manufacture of the NB964 filter, which made the LAGER project possible. We greatly appreciate the staff at NOAO/CTIO for their kind support to make our observations successful.

Based on observations at Cerro Tololo Inter-American Observatory, National Optical Astronomy Observatory (NOAO Prop. ID: 016A-0386, PI: Malhotra, and CN-TAC Prop. IDs: 2015B-0603 and 2016A-0610, PI: Infante), which is operated by the Association of Universities for Research in Astronomy (AURA) under a cooperative agreement with the National Science Foundation.

This project used data obtained with the Dark Energy Camera (DECam), which was constructed by the Dark Energy Survey (DES) collaboration. Funding for the DES Projects has been provided by the DOE and NSF (USA), MISE (Spain), STFC (UK), HEFCE (UK), NCSA (UIUC), KICP (U. Chicago), CCAPP (Ohio State), MIFPA (Texas A&M), CNPQ, FAPERJ, FINEP (Brazil), MINECO (Spain), DFG (Germany) and the collaborating institutions in the Dark Energy Survey, which are Argonne Lab, UC Santa Cruz, University of Cambridge, CIEMAT-Madrid, University of Chicago, University College London, DES-Brazil Consortium, University of Edinburgh, ETH Zurich, Fermilab, University of Illinois, ICE (IEEC-CSIC), IFAE Barcelona, Lawrence Berkeley Lab, LMU Munchen and the associated Excellence Cluster Universe, University of Michigan, NOAO, University of Nottingham, Ohio State University, University of Pennsylvania, University of Portsmouth, SLAC National Lab, Stanford University, University of Sussex, and Texas A&M University.

*Facilities:* Blanco (DECam)

## REFERENCES

- Annis, J., Soares-Santos, M., Strauss, M. A., et al. 2014, *ApJ*, 794, 120
- Bagley, M.B., Scarlata, C., Henry, A., et al. 2017, arXiv:1701.05193, accepted for *ApJ*
- Bertin, E. 2010, *Astrophysics Source Code Library*, ascl:1010.068
- Bolton, J. S., Haehnelt, M. G., Warren, S. J., et al. 2011, *MNRAS*, 416, L70
- Bouwens, R. J., Illingworth, G. D., Oesch, P. A., et al. 2015, *ApJ*, 803, 34
- Dijkstra, M., Wyithe, J. S. B., & Haiman, Z. 2007, *MNRAS*, 379, 253
- Fan, X., Strauss, M. A., Becker, R. H., et al. 2006, *AJ*, 132, 117
- Finkelstein, S. L.; Ryan, R. E., Jr.; Papovich, C., et al. 2015, *ApJ*, 810, 71
- Furlanetto, S. R., Zaldarriaga, M., & Hernquist, L. 2006, *MNRAS*, 365, 1012
- Gehrels, N. 1986, *ApJ*, 303, 336
- Haiman, Z., & Cen, R. 2005, *ApJ*, 623, 627
- Hibon, P., Cuby, J.-G., Willis, J., et al. 2010, *A&A*, 515, 97
- Hibon, P., Malhotra, S., Rhoads, J., & Willott, C. 2011, *ApJ*, 741, 101
- Hibon, P., Kashikawa, N., Willott, C., Iye, M., & Shibuya, T. 2012, *ApJ*, 744, 89
- Hu, E. M., Cowie, L. L., Barger, A. J., et al. 2010, *ApJ*, 725, 394
- Iye, M., Ota, K., Kashikawa, N., et al. 2006, *Nature*, 443, 186
- Jensen, H., Laursen, P., Mellema, G., et al. 2013, *MNRAS*, 428, 1366
- Kashikawa, N., Shimasaku, K., Matsuda, Y., et al. 2011, *ApJ*, 734, 119
- Konno, A., Ouchi, M., Ono, Y., et al. 2014, *ApJ*, 797, 16
- Krug, H.B., Veileux, S., Tilvi, V., et al. 2012, *ApJ*, 745, 122
- Malhotra, S., & Rhoads, J. E. 2006, *ApJ*, 647, L95
- Malhotra, S., & Rhoads, J. E. 2004, *ApJ*, 617, L5
- Matthee, J., Sobral, D., Santos, S., et al. 2015, *MNRAS*, 451, 400
- McQuinn, M., Hernquist, L., Zaldarriaga, M., & Dutta, S. 2007, *MNRAS*, 381, 75
- Muzzin, A., Marchesini, D., Stefanon, M., et al. 2013, *ApJS*, 206, 8
- Ota, K., Iye, M., Kashikawa, N., et al. 2008, *ApJ*, 677, 12-26
- Ota, K., Iye, M., Kashikawa, N., et al. 2010, *ApJ*, 722, 803
- Ouchi, M., Shimasaku, K., Akiyama, M., et al. 2008, *ApJS*, 176, 301-330
- Ouchi, M., Shimasaku, K., Furusawa, H., et al. 2010, *ApJ*, 723, 869
- Pentericci, L., Carniani, S., Castellano, M., et al. 2016, *ApJ*, 829, 11
- Planck Collaboration, Ade, P. A. R., Aghanim, N., et al. 2016, *A&A*, 594, A13
- Rhoads, J. E., Hibon, P., Malhotra, S., Cooper, M., & Weiner, B. 2012, *ApJ*, 752, L28
- Rhoads, J. E., & Malhotra, S. 2001, *ApJ*, 563, L5
- Santos, M. R. 2004, *MNRAS*, 349, 1137
- Santos, S., Sobral, D., & Matthee, J. 2016, *MNRAS*, 463, 1678
- Schenker, M. A., Ellis, R. S., Konidaris, N. P., & Stark, D. P. 2014, *ApJ*, 795, 20
- Shibuya, T., Kashikawa, N., Ota, K., et al. 2012, *ApJ*, 752, 114
- Stark, D. P., Richard, J., Charlot, S., et al. 2015, *MNRAS*, 450, 1846
- Stark, D. P., Ellis, R.S., Charlot, S., et al. 2017, *MNRAS*, 464, 469
- Stern, D., Yost, S. A., Eckart, M. E., et al. 2005, *ApJ*, 619, 12
- Tilvi, V., Rhoads, J.E., Hibon, P., et al. 2010, *ApJ*, 721, 1853
- Tilvi, V., Pirzkal, N., Malhotra, S., et al. 2016, *ApJ*, 827, 14
- Valdes, F., Gruendl, R., DES Project 2014, *ASPC*, 485, 379
- Willott, C. J., Carilli, C.L., Wagg, J., Wang, R. 2015, *ApJ*, 807, 180